Continuous High-Altitude Measurements of Cosmic Ray Neutrons and SEU/MCU at Various Locations: Correlation and Analyses Based-On MUSCA SEP^3

G. Hubert, R. Velazco, C. Federico, A. Cheminet, C. Silva-Cardenas, L. V. E. Caldas, F. Pancher, V. Lacoste, F. Palumbo, W. Mansour, L. Artola, F. Pineda, and S. Duzellier

***Abstract*—In this paper are described measurements at high-altitude of both radiation environment and effects. These measurements comprise cosmic ray neutrons and SBU/MCU on nanoscales devices. Results obtained at Pic-du-Midi, France, and in the city of Puno, Peru, are presented and analyzed. Analyses and cross comparisons based-on MUSCA SEP^3 calculations show a good agreement between experimental data and modeling, thus illustrating the importance of the knowledge of the radiation field for a reliable prediction.**

***Index Terms*—Atmospheric neutrons, multiple-cell upset (MCU), MUSCA SEP^3, neutron spectrometer, SBU/MCU board, single-event upset, SEU.**

I. Introduction

SINGLE-EVENT effects (SEEs) induced by particles (heavy ions, neutrons, protons,...) present in the space and atmospheric natural environments where electronics components operate are well known for many years. Neutrons and protons can indirectly induce errors by creating secondary ions following a nuclear reaction with the nucleus of the target. The carriers generated by primary or secondary ions are collected by the depletion region resulting in a current pulse. Recent papers [1]–[7] have confirmed the single-event upset (SEU) sensitivity of nanoscale devices to direct ionization by protons. Thus, in atmospheric natural environment, protons can induce directly errors in nanoscales devices.

Manuscript received September 24, 2012; revised December 04, 2012 and January 04, 2013; accepted January 10, 2013. Date of publication February 18, 2013; date of current version August 14, 2013.

G. Hubert, A. Cheminet, L. Artola, and S. Duzellier are with The French Aerospace Lab (ONERA), 31000 Toulouse, France (e-mail: guillaume.hubert@onera.fr; firstname.name@onera.fr).

R. Velazco; F. Pancher, and W. Mansour are with the TIMA Laboratory, 38031 Grenoble, France (e-mail: firstname.name@imag.fr).

C. Federico is with the Institute of Advanced Studies (IEAV), São José dos Campos 10906, Brazil (e-mail: claudiofederico@ieav.cta.br).

C. Silva-Cardenas is with the Pontificia Universidad Catolica del Peru (PUCP), Lima OH-45801, Peru (e-mail: csilva@pucp.edu.pe).

L. V. E. Caldas is with the Institute for Energetic and Nuclear Research (IPEN), São Paulo 05200, Brazil (e-mail: lcaldas@ipen.br).

V. Lacoste is with the French Institute for Radiological Protection and Nuclear Safety (IRSN), 13115 St. Paul-Lez-Durance, France (e-mail: Veronique.lacoste@irsn.fr).

F. Palumbo is with the Consejo Nacional de Investigaciones Cientificas (CNEA), Buenos Aires C1420, Argentina (e-mail: fefixpalumbo@cnea.gov.ar).

F. Pineda is with the University of Altiplano, Puno 33189, Peru (e-mail: ferpineda@gmail.com).

Color versions of one or more of the figures in this paper are available online at http://ieeexplore.ieee.org.

Digital Object Identifier 10.1109/TNS.2013.2240697

Particles from primary cosmic radiation (mainly protons) that hit the Earth's atmosphere give rise to a complex field of secondary particles. These particles include neutrons, protons, muons, pions, etc.

Electronic parts and systems are exposed to ionizing radiation fluxes that strongly depend on altitude, latitude, longitude, and the sun's activity. The causes of SEEs in nanoscale devices exposed to the atmospheric environment are neutrons, protons, and α-particles. Semiconductor device technologies scaling down to sub-90 nm induce new problems such as direct ionizing protons [1]–[7] and radial ionization profile effects on SEEs [8]–[10]. Thus, terrestrial neutrons and protons induced SEUs are one of such key issues that can be a major challenge to future nanometric technologies. Particularly, multicell upsets (MCUs), which are defined as simultaneous errors induced by a single event in more than one memory cell, are particularly investigated. Thus, soft error rate (SER) determination is still a challenge to evaluate the technology sensitivity and to extrapolate the trends for future generations of devices.

Different simulation and experimental approaches are in the literature to estimate the SER induced by terrestrial neutron environment: accelerated testing using alpha, neutron, or proton source/beams, real-time testing performed in the natural environments [11]–[17], and combination of experimental and simulation approaches [18]. An alternative approach consists in using the modeling at device and/or circuit level. Each approach has advantages and drawbacks.

In contrast with accelerated testing, which is relatively easy to perform, real-time testing is clearly time-consuming, although this strongly depends on the embedded capacity. Real-time tests appear as the unique experimental solution to accurately estimate the SER of the tested devices, ensuring that the test does not introduce artificial results. For example, the beam uniformity/fluctuations, the dosimetry errors, the chip orientation, or the limited representatively of the radiation field characteristics alter results and analyses.

Then, to estimate the SER in atmospheric environment, accelerated testing and simulation approaches do not allow for modeling the complexity and dynamics of the natural environment. Moreover, real-time tests performed in the natural environment provide an objective feedback about the SER obtained in a considered location. Coupled neutron/SEU measurements (including single-bit upset, SBU, and MCU) combined with the modeling approach allow performing a better analyses. This synergy can also help to develop an innovative methodology to evaluate the operational SBU/MCU risk.

Neutron spectrum measurement [19] and combination of neutron flux/spectrum measurement by using Bonner balls and soft-error rates have been performed [19]–[21]. Modeling approaches [22]–[26] have demonstrated a good agreement between high-altitude soft-error measurements and simulation results [23]. Then, some high-altitude campaigns dedicated to SER characterizations were achieved [12], [14], [16], [17].

Real-time SEU/MCU measurements have been performed since 2008 by ONERA and TIMA. They are done using an experimental platform including 1 Gb of SRAM built from two successive generations of commercial memories: 90- and 130-nm technologies. This platform was activated during commercial long-haul flights [11] and has flown as a piggyback experiment during balloon flights [27]. To complete these investigations, MUSCA SEP^3 calculations were performed and compared to experimental results [11], [27], [28]. Although these comparisons showed a satisfactory agreement, they have provided evidence for the significant importance of knowing and modeling the considered radiation environment. Furthermore, in 2011, the so-called HERMEIS neutron spectrometer [29]–[31] was installed by ONERA at Pic-du-Midi (2885 m, Midi-Pyrénées Observatory, OMP), France. The HERMEIS spectrometer is coupled with semiconductor detectors (pixel array and Si diodes) and a scintillator detector. The main objectives of these experiments are the characterization of the neutron field dynamics and the investigation of other particle fields such as protons and muons. The SRAM experimental platform complements this high-altitude experimental setup.

This paper presents a new collaborative TIMA-ONERA scientific thematic named Distributed Acquisitions in high-Altitude of Radiation Environment and SEE (DAARES). DAARES integrates coupled measurements of cosmic ray neutron fluxes/spectra and SEU occurring in nanoscales devices at different locations. The results obtained at Pic-du-Midi are presented and are complemented by data issued from the activation of the experimental platforms at a higher altitude (3889 m) in the city of Puno, Peru.

II. Experimental Platforms

In Fig. 1 are depicted both the high altitude sites in which are operating the experiments and the experimental platforms: the SRAM-board and the neutron detectors. As mentioned in the Introduction, coupled measurements are established thanks to scientific projects.

First is the DAARES project base on the Pic-du-Midi station, located in the French Pyrenees and which includes radiation field characterizations (neutron spectrometer and semiconductor detectors) and SEE measurements on the SRAM board. Second, there are the Puno experiments that are performed within the framework of the High Altitude Remotely Monitored Laboratory for the Evaluation of the Sensitivity to SEUs (HARMLESS) project[1].

[1]HARMLESS is a project started in 2011 in the frame of STIC-AmSud. The HARMLESS network includes partners from Peru, Brazil, Argentina, and France.

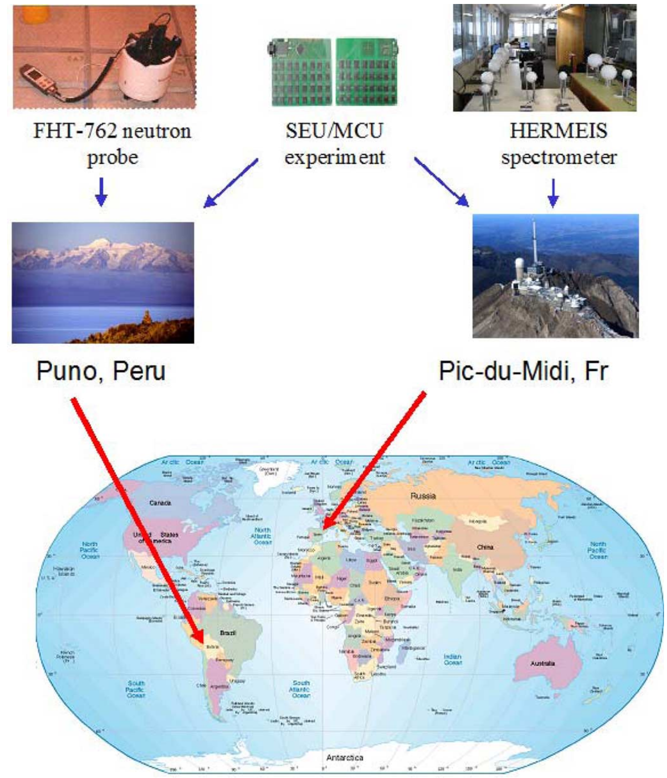

Fig. 1. SEU/MCU and neutron characterization experiments installed at Pic-du-Midi and Puno.

TABLE I
Characteristics of Both Altitude Locations

	Pic-du-Midi, France	Puno, Peru
Altitude (m)	2885	3889
Latitude	42°55'N	15°50'S
Longitude	0°08'E	70°01'W
Cut-off rigidity	5.6 GV	5 GV
Neutron flux relative to New York City	8.5	9
Neutron experiment	HERMEIS spectrometer	FHT 762 neutron probe
SEU experiment	2 Gbit 90nm SRAM	1 Gbit SRAM 130nm (704 Mb) / 90nm (320 Mb)
Start Operating	May 2011	March 2012

Thus, projects provide a very interesting measurement synergy that will be completed by a modeling approach based on the MUSCA SEP^3 platform. The next sections are devoted to describe the stations, the SEU experiment, then the neutron spectrometer/detector.

A. High Altitude Stations

The neutron radiation field characterization (fluxes and/or spectra) as well as SEU continuous measurements are simultaneously performed at the top of Pic-du-Midi and in the city of Puno. Table I summarizes the characteristics of these two sites.

Fig. 2. HERMEIS neutron spectrometer located in the Pic-du-Midi station (altitude, latitude, and longitude are respectively equal to 2.885 km, 42° 55′ N and 0° 08′ E).

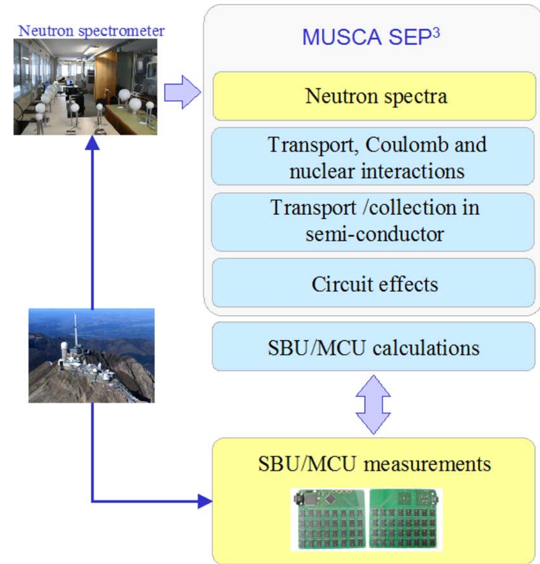

Fig. 3. Global methodology applied in this paper.

B. SEU Experiment

The experimental platform operating at Pic-du-Midi includes two SRAM boards (1 Gb each). The architecture of these boards was detailed in a previous work [11], [27], [28].

The board used for the Puno experiment is based on a similar design, but mixing SRAM chips issued from different technologies (130 and 90 nm) with, respectively, 704 and 320 Mb.

C. Neutron Detection Experiments

The neutron environment is measured at the Pic-du-Midi and the city of Puno using two distinct and complementary systems (see Fig. 1).

At the Pic-du-Midi station, the HERMEIS system, made of *Bonner multispheres*, is used [11]. HERMEIS (Fig. 2) was developed by the IRSN Laboratory of Neutron Metrology and Dosimetry and the Space Environment Department of ONERA (DESP), which has installed this spectrometer to study the dynamics of the energetic distributions, from meV to GeV, of cosmic-ray induced neutrons [30], [31]. Fig. 2 presents a photograph of the HERMEIS neutron spectrometer.

The HERMEIS neutron spectrometer consists of 10 homogeneous polyethylene (PE) spheres with increasing diameters (3, 3.5, 4, 4.5, 5, 6, 7, 8, 10, and 12 in). The high pressure (10 atm) ^{3}He spherical proportional counter (2 in) placed in the center of the spheres allows high detection efficiency. Additionally, the spectrometer includes two PE spheres with inner tungsten and lead shells (8 and 9in, respectively) in order to increase the response above 20 MeV. The counts given by each sphere are automatically stored every 5 min with the mean meteorological conditions. Then, in previous works [29]–[31], the fluence responses were calculated, and the method that allows for deducing the spectrum from detection levels was developed.

The neutron measurements performed at Puno were made with a *Thermo Scientific Monitor* composed by one ^{3}He proportional probe inserted inside a cylinder (tungsten and Polyethylene layers). Layers are specified to obtain the response for thermal neutrons up to 5 GeV [32]. This equipment allows for evaluating the dynamics of the neutron flux levels but not the spectra.

The calibrations of HERMEIS and the neutron detector were performed at CERF (CERN-EU high Energy Reference Field [33]) in order to ensure an appropriate response for the high-energy neutron field.

III. SEU Modeling and Global Methodology

The SEE prediction methodologies presented here aim at proposing suitable approaches for modern electronics. The rectangular parallelepiped (RPP) concept is largely used for microscales technological nodes and relies on the assumption that the deposited charge within a RPP volume provides a good description of the ion induced SEE mechanism.

Nowadays, device sensitive structures can no longer be represented in such a simplistic way because of their complex geometry, small dimensions, and close proximity with other adjacent sensitive zones. Moreover, the technological integration led to modify the collection mechanisms.

New methodologies based on multilevel physical approaches were proposed as a new paradigm [2], [34]–[46].

Among these methodologies, MUSCA SEP^3 first presented in 2009 [2] consists in modeling the whole device within its local and global environments and the detailed characteristics of the radiation field environment (nature, direction, and spectrum). Results presented in [2], [6], [47], and [48] have shown that each physical level is critical for SEE risk calculation including the environment description.

This paper provides the opportunity to simultaneously measure the neutron environment and the SEU response of nanoscales devices (see Fig. 3). The radiation field static and dynamic characteristics are monitored with a neutron spectrometer, while the 90-nm technological model has been developed and validated with technological analysis and SEU ground tests [27]. The 130-nm topology has been deduced from the 90 nm and based-on ITRS roadmap [49].

To define the technological models, reverse engineering process was performed [27]. This approach allows obtaining the critical technology parameters for the device model, such as

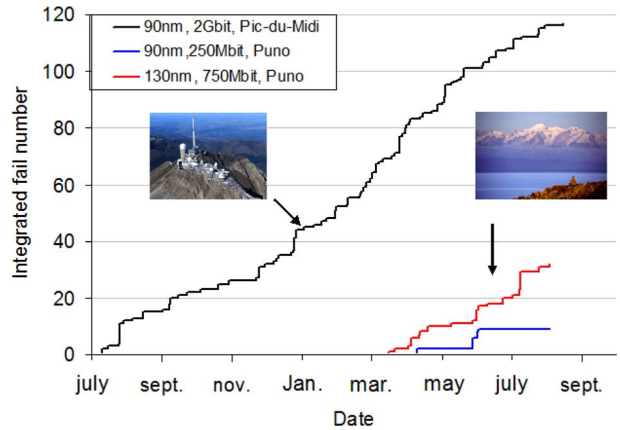

Fig. 4. SEU measurements in the Pic-du-Midi station and in Puno between July 2011 and August 2012.

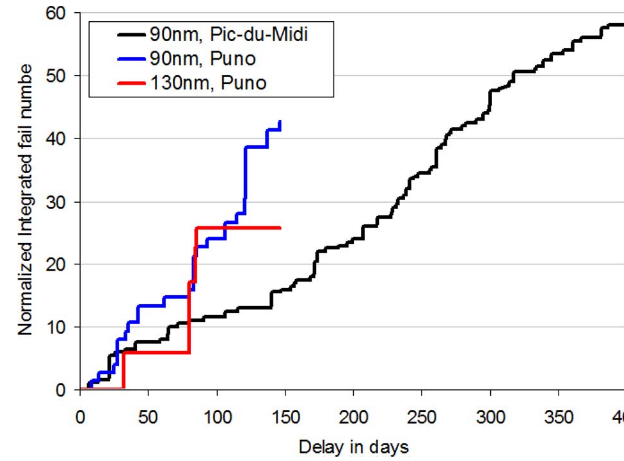

Fig. 5. Normalized SEU measurements (relative to time and the memory size) in the Pic-du-Midi station and in Puno.

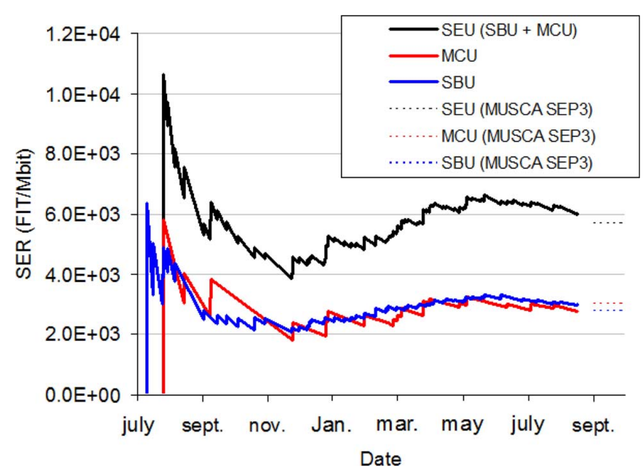

Fig. 6. Measured SER in FIT/Mb in Pic-du-Midi. Measurements performed between May 2011 and August 2012.

the topology of the SRAM cell, the dimensions of N and PMOS transistors, the description of the passivation layers, and the Shallow Trench Isolation (STI) details. In all the cases, the SEU occurrence model used by the predictive platform and based on critical charge concept needs to be adjusted and validated.

An interesting consequence of these experiments in the SEE modeling field is that the technological and SEE occurrence models can be optimized thanks to neutron and SEU measurements coupled with MUSCA SEP^3 analyses. To define the SEU occurrence model, radiation ground tests have been performed [27], and two different facilities were considered: the ILL, Grenoble, France, for thermal neutrons, and the KVI, Groningen, The Netherlands, for high-energy protons. Moreover, additional experimental data of neutron irradiation from ASP and TRIUMF facilities have been used [50]. Results issued from the ILL facility indicate a very low sensitivity to thermal neutron, i.e., there is not BPSG on the passivation layers.

Thus, models can be used for operational calculations considering complex geometries (i.e., cell topology, STI, passivation, and metallization layers).

IV. Results and Analyses

Fig. 4 proposes a summary of measurements (integrated fail number) performed in the Pic-du-Midi station and in Puno for both tested technologies. In the following, performed analyses and cross comparison will be presented.

Data acquisitions in the Pic-du-Midi were started in May 2011, and they allowed for obtaining a significant fail number (>100 SEUs). Moreover, measurements performed in Puno are more recent (March 2012), and the fail number, although significant for the 130 nm devices, induced several problems for analysis.

Fig. 5 presents the failure measurements normalized to the memory size and with the same initial time. This approach allows for comparing the relative sensitivity of tested memories and the effects related to test site conditions (location, altitude, ...). Results show that the 130-nm memory is more sensitive than the 90-nm one, and that the neutron field of Puno is higher than the Pic-du-Midi.

The following sections are devoted to present results and analyses and to propose a cross comparison of the data.

A. Results Obtained at Pic-du-Midi

The SEU platform and the neutron spectrometer are operational, respectively, since July and May 2011.

Typically, single event rate (SER) is measured in terms of failure in time (FIT), 1 FIT being a single failure in 10^9 device hours. A good practice consists in specifying the SER in FIT/Mb. Then, Fig. 6 presents the SER dynamics observed in the Pic-du-Midi, and results allow for distinguishing SBU and MCU events. SER levels are consistent with previous works [12]. The first MCU event was observed 10 days after the beginning of measurements.

In Fig. 7 are presented results analyzed from raw spectrometer measurements performed between May 2011 and August 2012. It is necessary to distinguish two periods resulting from the snow accumulation on the roof of the experimental room during the winter period (November 2011–March 2012) when the neutron spectrum is significantly attenuated.

The spectrum presented in Fig. 6 is issued from count rate data processing and results in an average spectrum. Results are compared to QARM [51]–[53] calculations.

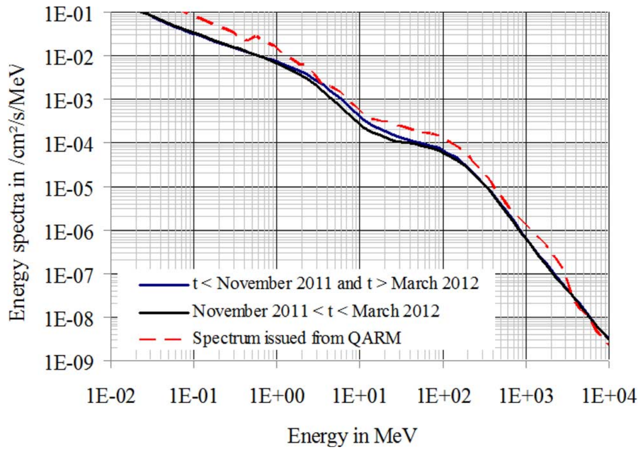

Fig. 7. Neutron energy spectra issued from QARM [51]–[53] and measured by HERMEIS at Pic-du-Midi between May 2011 and April 2012.

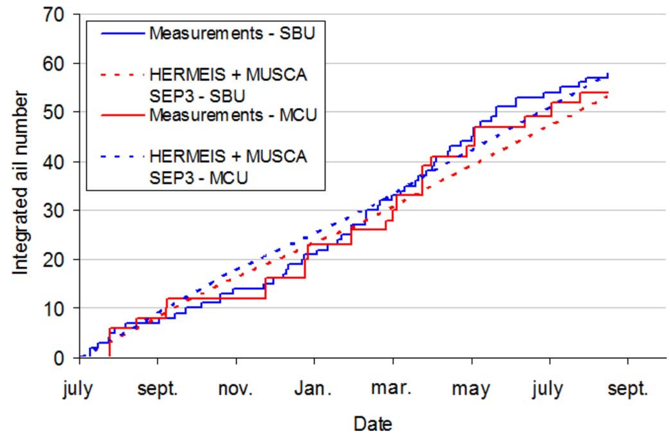

Fig. 9. Measured and calculated SEU events including the SBU and MCU events (MUSCA SEP^3 using the HERMEIS spectra as inputs).

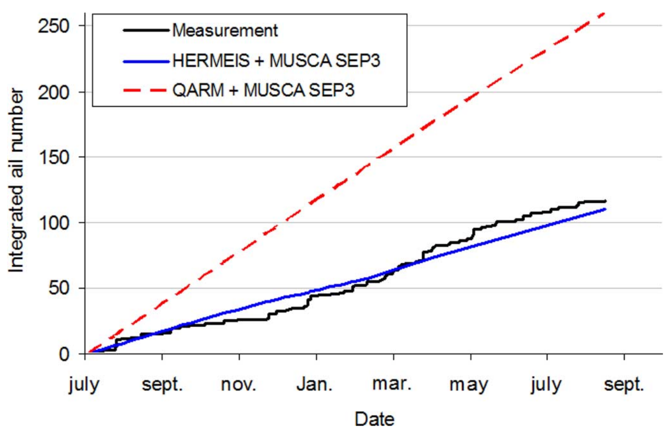

Fig. 8. Measured and calculated total events (MUSCA SEP^3 using the HERMEIS spectra and QARM as inputs).

TABLE II
EVENT MULTIPLICITY ISSUED FROM REAL-TIME EXPERIMENTS AND FROM MUSCA SEP^3 CALCULATIONS

Event type (SBU/MCU)	Measurements May 2011 → March 2011	Calculated event number (average value)
Total	83 SBU	73.7 SBU
SBU	41 SBU	38.3 SBU
MCU	42 SBU	35.4 SBU
2 bit	7 events → 50 %	54 %
3 bit	3 events → 21 %	22 %
4 bit	2 events → 14 %	13.8 %
5 bit	1 event → 7 %	6 %
6 bit	1 event → 7 %	3.5 %

The QARM results are obtained by considering the single position radiations service, the main used parameters being respectively the altitude (2.885 km), the latitude (42°55′N), and the longitude (0°08′E). In addition, input data consider the March 1, 2012 (median date), and input conditions consider GCR for incident spectrum and a Kp value equal to 2. Spectra resulting from QARM calculations correspond to average values and do not include variations. Otherwise, QARM spectrum corresponds to the sum of both up and down contributions.

Nevertheless, the HERMEIS spectrometer is able to monitor the neutron field with a dynamic in the hour scale. These hourly spectra are used to model the neutron field in MUSCA SEP^3.

Figs. 8 and 9 present the total and the SBU/MCU events measured, comparing them to the predicted rates. Fig. 8 presents some results: As mentioned, the integrated fail number is deduced from measurement and calculations, but calculations are performed considering spectra obtained respectively from the HERMEIS spectrometer (located close to the SEE experiment) and from the QARM calculations.

However, Fig. 8 provides evidence for the impact of our knowledge by the radiation field. Indeed, results issued form QARM overestimate (factor ~2.2) the experimental SER, while calculations integrating HERMEIS spectra are particularly relevant.

It is important to nuance the overestimate level. Indeed, the spectra deduced from QARM do not take into account the shielding provides by the mountain and structures (building). Moreover, calculations deduced from QARM spectrum consider the up contributions and the down contributions to the neutron spectra. Thus, this hypothesis overestimates the neutron field, and this can justify the overestimate factor observed, which reduces its real level. Nevertheless, this does not mean it takes into consideration only the down contribution of the neutron spectra. This analysis raises the interest of coupling high-altitude neutron spectrum and soft-error measurements.

Fig. 9 is particularly interesting because it allows for evaluating the modeling relevance as a function of event type (SBU or MCU). The comparison between the SBU and MCU modeling and measurements are very satisfactory. The MUSCA SEP^3 approach based on multilevel descriptions, i.e., the radiation field thanks to neutron spectrometer and the technology thanks SEE ground tests and analyses, is validated.

MCU results and agreement with modeling can be refined by performing multiplicity analyses. Measurements indicate a high proportion of MCU with multiplicity up to six (6 bit-flips due to a single particle were detected in March 2012). Table II presents predicted and measured event occurrences separating single and multiple events and specifying the event multiplicity.

Predicted MCU occurrences are consistent with measurements. However, the experimental statistics are insufficient for MCU of high multiplicity and can explain the difference (factor 2 underestimation for a multiplicity of 6). Furthermore, the 6-event may correspond to a rare failure mode such as SEUs

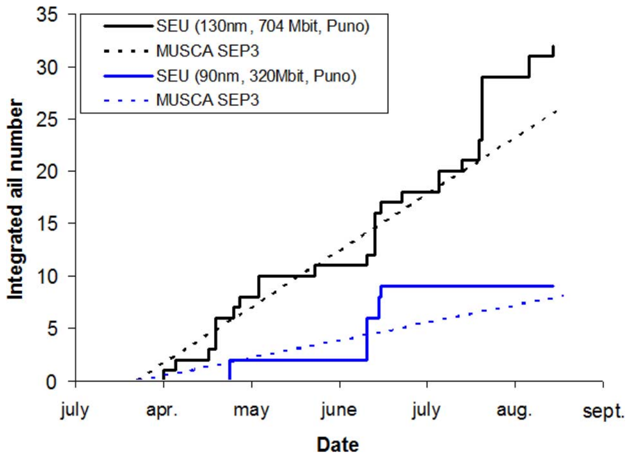

Fig. 10. Measured and calculated SBU/MCU events issued from 130- and 90-nm devices located in Puno.

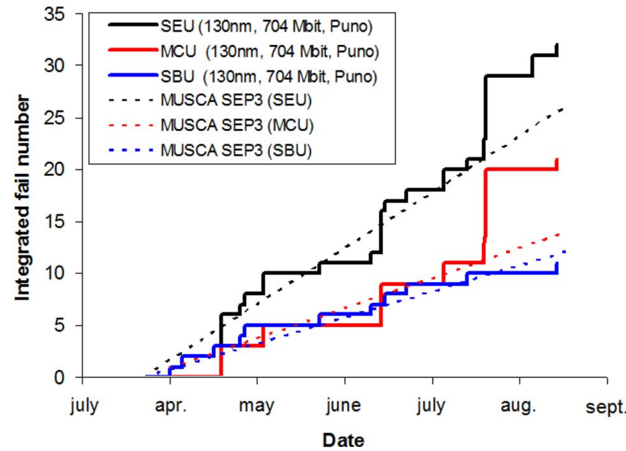

Fig. 11. Measured and calculated SBU/MCU events including the SBU and MCU events, 130-nm devices located in Puno.

TABLE III
NEUTRON FLUXES MEASURED IN PUNO VERSUS NYC REFERENCE

Location	Neutron Flux (n/cm2/s)	Relative to New York City
New York City, estimated for the same period and conditions, using the EXPACS code [18]	0.013	1
Puno - external	0.117 ± 0.011	9
Puno - internal	0.098 ± 0.011	7.5

in the peripheral part of the memory array (registers, address decoder, ...) [54]. Continuous monitoring is still ongoing and will allow improving these analyses.

Analyses based on the spectrum knowledge and MUSCA SEP^3 allow for investigating the neutron energy range contribution to SBU and MCU.

B. Results Obtained in Puno

Experiments in Puno have started in March 2012. Preliminary data allow for investigating the neutron flux at two positions: outdoors and indoors (plastic and glass roof) where the SRAM test platform is operating.

Table III summarizes the obtained fluxes and allows for estimating the accelerator factor with respect to the NYC reference.

The SEU measurement board, including SRAM parts issued from 130- and 90-nm technologies, is operational since March 2012. Fig. 10 presents respectively the measurements and the calculations issued from MUSCA SEP^3, which takes into account the neutron flux relative to New York City (see Table I) and the embedded capacities (respectively 2 Gb and 704 Mb).

Integrated fail number is relevant for the 130-nm technology, but insufficient for the 90-nm technology (9 SBU with a majority of MCU).

Calculations issued from MUSCA SEP^3 are relevant for the 130 nm. To model the neutron environment, we have considered respectively the flux level issued from the neutron detector measurements and the neutron spectrum shape deduced from HERMEIS measurements and analysis. Results presented in Figs. 10 and 11 show a good agreement, particularly when SBU and MCU events are discriminated.

Although results are correct for the 90-nm technology (Fig. 10), the numbers of observed upsets are not sufficient to perform an accurate comparison. However, orders of magnitude are consistent between the Pic-du-Midi and Puno data, and this reinforces our approach.

During the month of July, the measured MCU events significantly increased. This is not due to higher neutron flux levels, but rather to pure statistical effects.

The statistic effects induced by memory response variability were largely investigated in the past [15]–[17]. These analyses have shown that the shape of an upset cross-section curve is the result of a probability distribution that applies to all memory cells. This includes both the statistics of the primary or secondary energy deposition processes and the distribution of path lengths the ion may take through the sensitive cell. Moreover, the radiation field environment introduces an additional parameter to stochastic properties.

MUSCA SEP^3 approaches are based on average calculations, i.e., the sensitivity is deduced from the ratio between the SEE occurrence number and a large fluence, which represent a high number of random configurations.

Thus, calculations cannot consider the statistic effect, except from those induced by the environment dynamic. However, the dynamic measurement, performed thanks to the thermo scientific monitor, does not indicate a significant neutron flux increase. In July 2012, two MCU events were observed. These events were characterized by a multiplicity respectively equal to 2 and 6.

C. Synthesis of Results and Cross-Comparison

To synthesize the results, Figs. 12 and 13 present the calculated and the measured SER (in terms of FIT/Mb) obtained respectively in the Pic-du-Midi and Puno, but also for both devices.

These two figures illustrate the excellence of data issued from Pic-du-Midi, especially for the SBU and MCU analyses. Globally, Fig. 12 shows an acceptable agreement when all events are considered (SBU and MCU).

Moreover, cross comparisons show that 130-nm devices are more sensitive to radiation effects than 90-nm devices (Puno

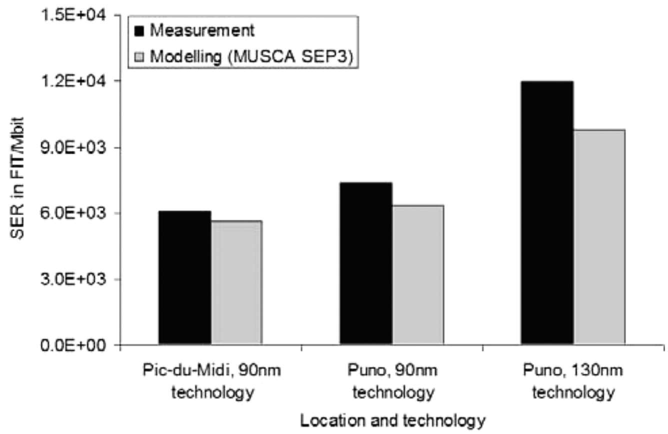

Fig. 12. Comparison between the measured and calculated total SER in FIT/Mb for the 90- and the 130-nm devices and for both high-altitude locations (Pic-du-Midi and Puno).

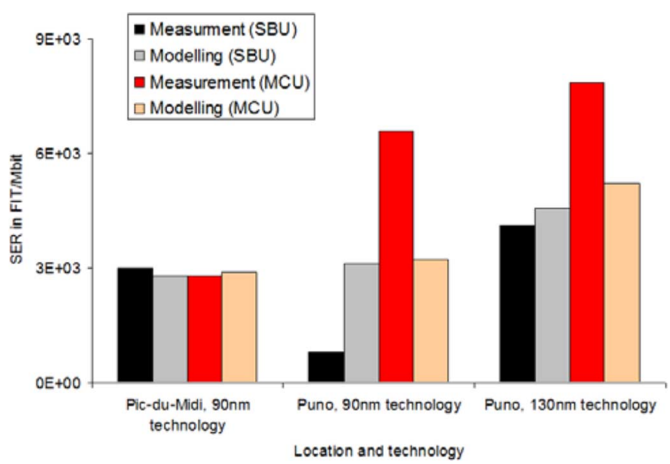

Fig. 13. Comparison between the measured and calculated SER (distinguishing the SBU and MCU events) for the 90- and the 130-nm devices and for both high-altitude locations (Pic-du-Midi and Puno).

results), proving also that the radiation field at Puno is slightly more important than the one at Pic-du-Midi. This is conformal to Neutron fluxes relative to New York City (presented in Table I, i.e., the characteristics of both altitude locations) and issued from calculations.

Results presented in Fig. 13 allow for identifying some anomalies, among which are the measured and calculated MCU SER. As previously mentioned, results obtained for the 90-nm devices are statistically insufficient, but results will refine it over time exposition.

The results obtained in Puno for 130-nm SRAMs are very interesting, particularly the difference observed for MCU events. Indeed, a high multiplicity error (certainly due to the impact of a single particle, 6 SBU) was detected on July 22 and had a significant impact on analyses.

V. Conclusion and Perspectives

This paper presents test platforms and experimental data issued from simultaneous and continuous measurements coupling SEU and neutron dynamics in high altitude. Results obtained at the sites where the platforms were activated (Pic-du-Midi station and Puno) were presented in detail. These coupled measurements are integrated in the framework of in two international projects (HARMLESS and DAARES).

A very good agreement is observed between measurements performed at the two considered sites and calculations issued from MUSCA SEP^3. Compared to previous work [11], [27], [28], the agreement is improved and reinforces the fact that the radiation field knowledge is a key issue for predictive approaches on nanoscales devices. In addition, results demonstrate the relevance of modeling for the SBU and MCU analyses.

An important aspect of this work is the end-user approach. Indeed, the SRAM boards are based on commercial devices whose details are initially unknown. Thus, few SEE ground tests and technological analyses are sufficient to develop relevant models used in MUSCA SEP^3.

As a conclusion, high-altitude stations, i.e., the Pic-du-Midi and Puno, dedicated to online SEE and neutron measurements allow for proposing a synergy between SEE measurements, radiation field characterizations and SEE modeling. This synergy constitutes a relevant way to evaluate and to investigate the SEE trends for nanoscales devices, and furthermore it will allow for anticipating the SEE trends.

An important perspective consists in extending our approach according to two complementary ways: on the one hand to explore other locations (high altitude or magnetic anomaly as the South Atlantic Anomaly and high geomagnetic latitude environments), and on the other hand to develop new SRAM boards embedding more integrated devices.

New measurements began in 2012 in the Aiguille-du-Midi (French Alpes), and some SBUs and MCUs occurred. Moreover, new SRAM boards, built from SRAM devices in 65 nm, are in progress and will be operational at the end of 2012.

References

[1] D. F. Heidel, P. W. Marshall, K. A. LaBel, J. R. Schwank, K. P. Rodbell, M. C. Hakey, M. D. Berg, P. E. Dodd, M. R. Friendlich, A. D. Phan, C. M. Seidleck, M. R. Shaneyfelt, and M. A. Xapsos, "Low energy proton single-event-upset test results on 65 nm SOI SRAM," *IEEE Trans. Nucl. Sci.*, vol. 55, no. 6, pp. 3394–3400, Dec. 2008.

[2] G. Hubert, S. Duzellier, C. Inguimbert, C. Boatella-Polo, F. Bezerra, and R. Ecoffet, "Operational SER calculations on the SAC-C orbit using the Multi SCAles single event phenomena predictive platform (MUSCA SEP3)," *IEEE Trans. Nucl. Sci.*, vol. 56, no. 6, pp. 3032–3042, Dec. 2009.

[3] D. F. Heidel, K. P. Rodbell, E. H. Cannon, C. Cabral, Jr., M. S. Gordon, P. Oldiges, and H. H. K. Tang, "Alpha-particle-induced upsets in advanced CMOS circuits and technology," *IBM J. Res. Dev.*, vol. 52, no. 3, pp. 225–232, 2008.

[4] D. F. Heidel, P. W. Marshall, J. A. Pellish, K. P. Rodbell, K. A. LaBel, J. R. Schwank, S. E. Rauch, M. C. Hakey, M. D. Berg, C. M. Castaneda, P. E. Dodd, M. R. Friendlich, A. D. Phan, C. M. Siedleck, M. R. Shaneyfelt, and M. A. Xapsos, "Single-event upsets and multiple-bit upsets on a 45 nm SOI SRAM," *IEEE Trans. Nucl. Sci.*, vol. 56, no. 6, pp. 3499–3504, Dec. 2009.

[5] R. K. Lawrence, J. F. Ross, N. F. Haddad, R. A. Reed, and D. R. Albrecht, "Soft error sensitivities in 90 nm bulk CMOS SRAMs," in *Proc. Radiation Effects Data Workshop, NSREC*, 2009, pp. 71–75.

[6] G. Hubert, S. Duzellier, C. Boatella-Polo, F. Bezerra, and R. Ecoffet, "MUSCA SEP^3 contributions to investigate the direct ionization proton upset in 65 nm technology for space, atmospheric and ground applications," in *Proc. RADECS*, 2009, pp. 179–186.

[7] B. D. Siervawski, J. A. Pellish, R. A. Reed, R. D. Schrimpf, K. M. Warren, R. A. Weller, M. H. Mendenhall, J. D. Black, A. D. Tipton, M. A. Xapsos, R. C. Baumann, X. Deng, M. J. Campola, M. R. Friendlich, H. S. Kim, A. M. Phan, and C. M. Seidleck, "Impact of low-energy proton induced upsets on test methods and rate predictions," *IEEE Trans. Nucl. Sci.*, vol. 56, no. 6, pp. 3085–3092, Dec. 2009.

[8] M. Raine, G. Hubert, M. Gaillardin, L. Artola, P. Paillet, S. Girard, J.-E. Sauvestre, and A. Bournel, "Impact of the radial ionization profile on SEE prediction for SOI transistors and SRAMs beyond the 32-nm technological node," *IEEE Trans. Nucl. Sci.*, vol. 58, no. 3, pp. 840–847, Jun. 2011.

[9] M. Raine, G. Hubert, M. Gaillardin, P. Paillet, and A. Bournel, "Implementing realistic heavy ion tracks in a SEE prediction tool: Comparison between different approaches," *IEEE Trans. Nucl. Sci.*, vol. 59, no. 4, pp. 950–957, Aug. 2012.

[10] M. Raine, G. Hubert, M. Gaillardin, P. Paillet, and A. Bournel, "Monte Carlo prediction of heavy ion induced MBU sensitivity for SOI SRAMs using radial ionization profile," *IEEE Trans. Nucl. Sci.*, vol. 58, no. 6, pp. 2607–2613, Dec. 2011.

[11] P. Peronnard, R. Velazco, and G. Hubert, "Real-life SEU experiments on 90 nm SRAMs in atmospheric environment: Measures vs. predictions done by means of MUSCA SEP3 platform," *IEEE Trans. Nucl. Sci.*, vol. 56, no. 6, pp. 3450–3455, Dec. 2009.

[12] H. Puchner, "Correlation of life testing to accelerated soft error testing," in *Proc. 3rd Annu. IEEE SER Workshop*, San Jose, CA, USA, 2011, pp. 1–23.

[13] T. Sato and K. Niita, "Analytical functions to predict cosmic-ray neutron spectra in the atmosphere," *Radiat. Res.*, vol. 166, pp. 544–555, 2006.

[14] J.-L. Autran, P. Roche, J. Borel, C. Sudre, K. Castellani-Coulié, D. Munteanu, T. Parrassin, G. Gasiot, and J.-P. Schoellkopf, "Altitude SEE test European platform (ASTEP) and first results in CMOS 130 nm SRAM," *IEEE Trans. Nucl. Sci.*, vol. 54, no. 4, pp. 1002–1009, Aug. 2007.

[15] Z. Torok, S. P. Platt, and X. X. Cai, "SEE-inducing effects of cosmic rays at the high-altitude research station Jungfraujoch compared to accelerated test data," in *Proc. 9th Eur. Conf. RADECS*, 2007, pp. 1–6.

[16] A. Lesea and J. Fabura, "The Rosetta experiment: Atmospheric soft error rate testing in differing technology FPGAs," SELSE II, Urbana-Champaign, IL, Apr. 11–12, 2006.

[17] A. Lesea and J. Fabula, "Continuing experiments on atmospheric neutron effects on deep sub-micron integrated circuits," in *Proc. Workshop Radiation Effects Compon. Syst.*, Athens, Greece, Sep. 27–29, 2006, No. D-4.

[18] M. B. Chadwick and E. Normand, "Use of new ENDF/B-VI proton and neutron cross section for single event upset calculations," *IEEE Trans. Nucl. Sci.*, vol. 46, no. 6, p. 1386, Dec. 1999.

[19] T. Nakamura, M. Baba, E. Ibe, Y. Yahagi, and H. Kameyama, *Terrestrial Neutron-Induced Soft-Errors in Advanced Memory Devices*. Hackensack, NJ, USA: World Scientific, 2008.

[20] Y. Tosaka, R. Takasu, T. Uemura, H. Ehara, H. Matsuyama, S. Satoh, A. Kawai, and M. Hayashi, National Astronomical Observatory of Japan, Tokyo, Japan, "Simultaneous measurement of soft error rate of 90 nm CMOS SRAM and cosmic ray neutron spectra at the summit of Mauna Kea," in *Proc. IRPS*, Anaheim, CA, USA, Apr. 15–19, 2008, pp. 727–728, No. SE01.

[21] H. Kameyama, Y. Yahagi, and E. Ibe, "A quantitative analysis of neutron-induced multi-cell upset in deep sub micron SRAMs and of the impact due to anomalous noise," in *Proc. 45th Int. Rel. Phys. Symp.*, Phoenix, AZ, USA, Apr. 15–19, 2007, pp. 678–679.

[22] E. Ibe, "Current and future trend on cosmic-ray-neutron induced single event upset at the ground down to 0.1-micron-device," in *Proc. Svedberg Lab. Workshop Appl. Phys.*, Uppsala, Sweden, May 3, 2001, No. 1.

[23] E. Ibe, Y. Yahagi, F. Kataoka, Y. Saito, A. Eto, and M. Sato, "A self-consistent integrated system for terrestrial-neutron induced single event upset of semiconductor devices at the ground," in *Proc. ICITA*, Bathurst, Australia, Nov. 25–28, 2002, No. 273-21.

[24] E. Ibe, Y. Yahagi, H. Yamaguchi, and H. Kameyama, "SEALER: Novel Monte-Carlo simulator for single event effects of composite-materials semiconductor devices," in *Proc. RADECS*, Sep. 19–23, 2005, No. E-4.

[25] E. Ibe, S. Chung, S. Wen, H. Yamaguchi, Y. Yahagi, H. Kameyama, S. Yamamoto, and T. Akioka, "Spreading diversity in multi-cell neutron-induced upsets with device scaling," in *Proc. CICC*, San Jose, CA, USA, Sep. 10–13, 2006, pp. 437–444.

[26] E. Ibe, H. Taniguchi, Y. Yahagi, K. Shimbo, and T. Toba, "Impact of scaling on neutron-induced soft error in SRAMs from a 250 nm to a 22 nm design rule," *IEEE Trans. Electron Devices*, vol. 57, no. 7, pp. 1527–1538, Jul. 2010.

[27] L. Artola, R. Velazco, G. Hubert, S. Duzellier, T. Nuns, B. Guerard, P. Peronnard, W. Mansour, F. Pancher, and F. Bezerra, "In flight SEU/MCU sensitivity of commercial nanometric SRAMs: Operational estimations," *IEEE Trans. Nucl. Sci.*, vol. 57, no. 6, pp. 2644–2651, Dec. 2011.

[28] G. Hubert, R. Velazco, and P. Peronnard, "A generic platform for remote accelerated tests and high altitude SEU experiments on advanced ICs: Correlation with MUSCA SEP3 calculation," in *Proc. IEEE Int. On-Line Testing Symp.*, Jun. 2009, pp. 180–180.

[29] A. Cheminet, V. Lacoste, V. Gressier, G. Hubert, A. Martin, and M. Pépino, "Characterization of the IRSN neutron multisphere spectrometer (HERMEIS) at European standard calibration fields," *J. Instrum., 2nd FNDA*, vol. 7, 2012.

[30] A. Cheminet, G. Hubert, V. Lacoste, R. Velazco, and D. Boscher, "Characterization of the neutron environment and SEE investigations at the CERN-EU high energy reference field and at the Pic du Midi," in *Proc. RADECS*, 2012, submitted for publication.

[31] A. Cheminet, V. Lacoste, G. Hubert, D. Boscher, D. Boyer, and J. Pouponney, "Experimental measurements of the neutron fluence energy distributions at various mountain altitudes with HERMEIS," *IEEE Trans. Nucl. Sci.*, vol. 59, no. 4, pp. 1722–1730, Aug. 2012.

[32] "Thermo-scientific, FHT 762-Wendi-2 datasheet," (n.42540/85 TD-E), 2012.

[33] A. Mitaroff and M. Silari, "The CERN-EU high-energy reference field (CERF) facility for dosimetry at commercial flight altitudes and in space," *Radiat. Prot. Dosim.*, vol. 102, no. 1, pp. 7–22, 2002.

[34] H. H. K. Tang and E. H. Cannon, "SEMM–2: A modelling system for single event upset analysis," *IEEE Trans. Nucl. Sci.*, vol. 51, no. 6, pp. 3342–3348, Dec. 2004.

[35] K. M. Warren, R. A. Weller, B. D. Sierawski, R. A. Reed, M. H. Mendenhall, R. D. Schrimpf, L. W. Massengill, M. E. Porter, J. D. Wilkinson, K. A. LaBel, and J. H. Adams, "Application of RADSAFE to model the single event upset response of a 0.25 μm CMOS SRAM," *IEEE Trans. Nucl. Sci.*, vol. 54, no. 4, pp. 898–903, Aug. 2007.

[36] Y. Tosaka, H. Kanata, T. Itakura, and S. Satoh, "Simulation technologies for cosmic ray neutron-induced soft errors: Models and simulation systems," *IEEE Trans. Nucl. Sci.*, vol. 46, no. 3, pp. 774–780, Jun. 1999.

[37] K. M. Warren, B. D. Sierawski, R. A. Reed, R. A. Weller, C. Carmichael, A. Lesea, M. H. Mendenhall, P. E. Dodd, R. D. Schrimpf, L. W. Massengill, T. Hoang, H. Wan, J. L. De Jong, R. Padovani, and J. J. Fabula, "Monte-Carlo based on-orbit single event upset rate prediction for a radiation hardened by design latch," *IEEE Trans. Nucl. Sci.*, vol. 54, no. 6, pp. 2419–2425, Dec. 2007.

[38] K. M. Warren, A. L. Sternberg, R. A. Weller, M. P. Baze, L. W. Massengill, R. A. Reed, M. H. Mendenhall, and R. D. Schrimpf, "Integrating circuit level simulation and Monte-Carlo radiation transport code for single event upset analysis in SEU hardened circuitry," *IEEE Trans. Nucl. Sci.*, vol. 55, no. 6, pp. 2886–2894, Dec. 2008.

[39] K. M. Warren, J. D. Wilkinson, R. A. Weller, B. D. Sierawski, R. A. Reed, M. E. Porter, M. H. Mendenhall, R. D. Schrimpf, and L. W. Massengill, "Predicting neutron induced soft error rates: Evaluation of accelerated ground based test methods," in *Proc. IEEE 46th Annu. Int. Rel. Phys. Symp.*, Phoenix, AZ, USA, 2008, pp. 473–477.

[40] G. Hubert, J.-M. Palau, K. Castellani-Coulie, M.-C. Calvet, and S. Fourtine, "Detailed analysis of secondary ions effects for the calculation of neutron-induced SER in SRAMs," *IEEE Trans. Nucl. Sci.*, vol. 48, no. 6, pp. 1953–1959, Dec. 2001.

[41] G. Hubert, N. Buard, C. Weulersse, T. Carriere, M.-C. Palau, J.-M. Palau, D. Lambert, J. Baggio, F. Wrobel, F. Saigne, and R. Gaillard, "Review of DASIE family code: Contribution to SEU/MBU understanding," in *Proc. 11th IEEE Int. On-Line Testing Symp.*, 2005, pp. 87–94.

[42] R. A. Weller, R. A. Reed, K. M. Warren, M. H. Mendenhall, B. D. Sierawski, R. D. Schrimpf, and L. W. Massengill, "General framework for single event effects rate prediction in microelectronics," *IEEE Trans. Nucl. Sci.*, vol. 56, no. 6, pp. 3098–3108, Dec. 2009.

[43] R. A. Weller, M. H. Mendenhall, R. A. Reed, R. D. Schrimpf, K. W. Warren, B. D. Sierawski, and L. W. Massengill, "Monte Carlo simulation of single event effects," *IEEE Trans. Nucl. Sci.*, vol. 57, no. 4, pp. 1726–1746, Aug. 2010.

[44] F. Wrobel, G. Hubert, and P. Iacconi, "A semi-empirical approach for heavy ion SEU cross section calculations," *IEEE Trans. Nucl. Sci.*, vol. 53, no. 6, pt. 1, pp. 3271–3276, Dec. 2006.

[45] D. Lambert, J. Baggio, G. Hubert, V. Ferlet-Cavrois, O. Flament, F. Saigne, F. Wrobel, H. Duarte, J. Boch, B. Sagnes, N. Buard, and T. Carriere, "Neutrin-induced SEU in SRAMs: Simulations with n-Si and n-O interactions," *IEEE Trans. Nucl. Sci.*, vol. 52, no. 6, pp. 2332–2339, Dec. 2005.

[46] S. Uznanski, G. Gasiot, P. Roche, C. Tavernier, and J.-L. Autran, "Single event upset and multiple cell upset modeling in commercial bulk 65-nm CMOS SRAMs and flip-flops," *IEEE Trans. Nucl. Sci.*, vol. 57, no. 4, pp. 1876–1883, Aug. 2010.

[47] G. Hubert, S. Bourdarie, L. Artola, S. Duzellier, C. Boattela-Polo, F. Bezerra, and R. Ecoffet, "Impact of the solar flares on the SER dynamics on micro and nanometric technologies," *IEEE Trans. Nucl. Sci.*, vol. 57, no. 6, pp. 3127–3134, Dec. 2010.

[48] G. Hubert, S. Bourdarie, L. Artola, S. Duzellier, C. Boattela-Polo, F. Bezerra, and R. Ecoffet, "Operational risk assessment at solar events using a new statistical approach for SEU rate prediction," in *Proc. NSREC*, 2012.

[49] "International Technology Roadmap for Semiconductor," 2006.

[50] A. Hands, P. Morris, C. Dyer, K. Ryden, and P. Truscoot, "Single event effects in power MOSFETs and SRAMs due to 3 MeV, 14 MeV and fission neutrons," *IEEE Trans. Nucl. Sci.*, vol. 58, no. 3, pp. 952–959, Jun. 2011.

[51] "QARM, Qinetiq Atmospheric Radiation Model," [Online]. Available: http://qarm.space.qinetiq.com

[52] F. Lei *et al.*, "An atmospheric radiation model based on response matrices generated by detailed Monte-Carlo simulations of cosmics rays interactions," *IEEE Trans. Nucl. Sci.*, vol. 51, no. 6, pp. 3442–3451, Dec. 2004.

[53] F. Lei, A. Hands, S. Clucas, C. Dyer, and P. Truscott, "Improvement to and validations of the QinetiQ atmospheric radiation model (QARM)," *IEEE Trans. Nucl. Sci.*, vol. 53, no. 4, pp. 1851–1858, Aug. 2006.

[54] G. Hubert, S. Bourdarie, R. Velazco, S. Duzellier, L. Artola, and R. Ecoffet, "Operational risk assessment at solar events using a new statistical approach for SEU rate prediction," in *Proc. NSREC*, 2012.